An Investigation of Frictionless Enveloping Grasping in the Plane

Jeffrey C. Trinkle
GRASP Laboratory
Department of Systems Engineering
University of Pennsylvania
Philadelphia, Pennsylvania 19104

Jacob M. Abel
Department of Mechanical Engineering
and Applied Mechanics
University of Pennsylvania
Philadelphia, Pennsylvania 19104

Richard P. Paul
GRASP Laboratory
Department of Computer and Information Science
University of Pennsylvania
Philadelphia, Pennsylvania 19104

Abstract

Grasping by a two-dimensional hand composed of a palm and two hinged fingers is studied. The mathematics of frictionless grasping is presented and used in the development of a planner/simulator. The simulator computes the motion of the object using an active constraint set method and assuming exact knowledge of the physical properties of the polygonal object, hand, and support. Grasping is divided into three phases. During the first phase, the initial grasping configuration is found. In the second phase, the object is manipulated away from the support, bringing it into contact with the palm. In the last phase, the grip is adjusted to minimize the contact forces acting on the object.

This research was supported by the following grants: IBM 6-28270, ARO DAA6-29-84-k-0061, AfOSR 82-NM-299, NSF ECS 8411879, NSF MCS-8219196-CER, NSF MCS 82-07294, AVRO DAABO7-84-K-FO77, and NIH 1-RO1-HL-29985-01. Any opinions, findings, conclusions, or recommendations expressed in this publication are those of the authors and do not necessarily reflect the views of the granting agencies.

The International Journal of Robotics Research,
Vol. 7, No. 3, June 1988,

1. Introduction

Flexible manufacturing workcells typically contain a robot arm and many expensive, special-purpose, end-of-arm tools. The potential for cost and time savings through the use of a general-purpose hand has fueled much research in the last 10 years on designing, analyzing, and programming articulated mechanical hands (Hanafusa and Asada 1982; Okada 1982; Salisbury 1982; Kerr 1984; Kobayashi 1984; Cutkosky 1985; Holzmann and McCarthy 1985; Juan and Paul 1986). Most studies have proceeded under the assumption that contact friction forces will be large enough to keep the object from sliding on the fingers. In contrast, this paper is concerned with the mechanical analysis of "hands" when the friction forces are not large enough to prevent sliding. The results are applied to planning grasps using the surfaces of the hand, not just the fingertips.

Previous Work

The potential for grasping and manipulating a wide variety of objects with a single end-effector has en-

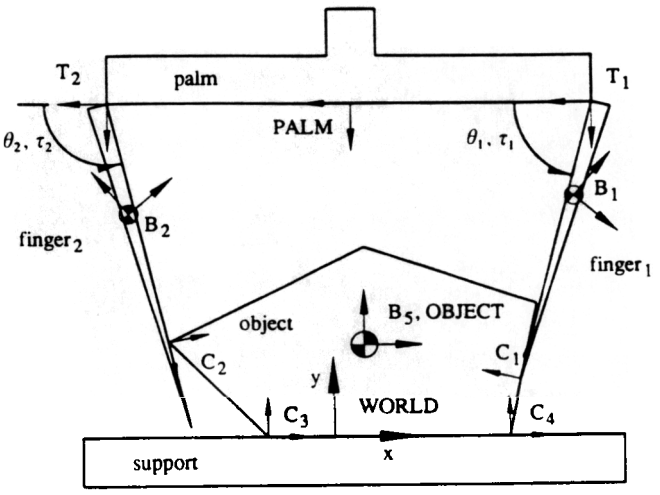

Fig. 1. A typical hand in an initial grasping configuration.

couraged research in grasp mechanics as well as in sensing and hand programming. Salisbury (1982) studied the mechanics of fingertip grasps under the assumptions of rigid-body kinematics and coulomb friction. For an object held in tip prehension, he developed a method to control the hand to impart small arbitrary motions and apply arbitrary forces to the object. He also developed a method to control the effective Cartesian stiffness of the grasped object. Cutkosky (1985) included the effects of the curvature of the fingertips and the structural stiffness of the fingers. Central to Salisbury's formulation is the hand's ability to apply normal forces to the object that are large enough to prevent slipping between the object and any finger. Since slipping cannot always be prevented, Holzmann and McCarthy (1985) developed a method to predict slipping and the accompanying friction forces.

There are an infinite number of possible grasps of an object. Jameson (1985) applied numerical optimization techniques to choose a three-point grasp that provided complete rigid restraint of the object relative to the hand. Hanafusa and Asada (1982) developed a hand with flexible fingers to pick up planar objects. They derived stability conditions and grasp-selection criteria based on minimizing the potential energy of the fingers. Others have applied optimization techniques to various objective functions to choose "optimal" grasps (Boissonnat 1982; Kobayashi 1984; Hanafusa 1985; Jameson 1985; Nguyen 1985; Trinkle 1985).

A very difficult area of grasping research is planning. Planning grasps for articulated mechanical hands is computationally expensive. Perhaps this is why the only work to date is for grippers with prismatic joints. Laugier and Wolter (Laugier and Pertin 1983; Wolter et al. 1984) both plan grasps by considering the volume swept out by a parallel-jawed gripper in its approach to an object. Juan (Juan and Paul 1986) built an interactive system, PAAR, to aid planning assembly tasks. Extending Mason's (1984) work in manipulation, Brost (1985) developed a technique for planning grasps of polygons that were free to slide on a supporting plane.

The most mathematically complex aspect of grasping is in the manipulation of the grasped object over a large range. Okada (1982) programmed a hand with three fingers and 11 degrees of freedom to turn a nut onto a bolt. Such successes are few because the equations describing manipulation are differential, nonlinear, time-varying, and constrained (Kerr 1984).

.2. Problem Statement

The problem addressed is that of picking up an object with an articulated mechanical hand in the absence of friction. It has been shown by Lakshminarayana (1978) that if a frictionless grasp is used to completely restrain an object, using only fingertips, a hand would need a minimum of seven fingers (four in the two-dimensional case). However, the necessary number of fingers may be reduced to three (two in the plane) if the hand's entire palmar surface is used[1] (this includes the palm and those surfaces of the fingers that face the palm).

.3. Assumptions

A typical two-dimensional "hand" is shown in Fig. 1. There are two single-link fingers (bodies 1 and 2) and

[1] This idea was proposed by R. Bajcsy.

a flat palm. The object (body 5) is initially at rest on the support, which is fixed in the world. The x- and y-axes of the world coordinate frame define the plane of interest. All moments and rotations have nonzero components in the z-direction (out of the page). For the mathematical analysis presented in Section 2, we make the following assumptions:

1. the fingers and hand move under exact position control,
2. all bodies are rigid convex polygons,
3. the mass and the position of the center of gravity of each body is known,
4. the kinematic arrangement of the hand is known,
5. the motion proceeds slowly enough to ignore dynamic effects,
6. there are no friction forces acting on the bodies, and
7. the object is initially at rest in a known position on the supporting surface.

As a direct result of the second assumption, we know that for any pair of contacting bodies, the contact occurs either at a point or along a line segment. A line segment contact is treated as two point contacts, one at each end of the segment. This assumption allows for the uniform treatment of all contacts while maintaining the correct kinematic constraints (Featherstone 1985).

.4. Notation and Conventions

The notation and conventions used in this paper are as follows: vectors are indicated by boldface, lowercase letters (e.g., $\mathbf{x}$); circumflex, $\hat{\mathbf{x}}$, is used to denote unit vectors; matrices are boldface, uppercase letters (e.g., $\mathbf{A}$); a dagger superscript, $\mathbf{A}\dagger$, denotes the pseudoinverse of the matrix; a matrix $\mathbf{A}$ or vector $\mathbf{x}$ defined with respect to a coordinate frame $\mathbf{B}$ is written as ${}^{\mathbf{B}}\mathbf{A}$ or ${}^{\mathbf{B}}\mathbf{x}$, respectively (if $\mathbf{B}$ is the world frame, the superscript is absent); a dot, $\dot{\mathbf{x}}$, over a variable implies its time derivative; $\mathbf{A}^{\mathbf{T}}$ is the transpose of $\mathbf{A}$; and the subscripts x, y, z when applied to a vector indicate one of its components (e.g., $\mathbf{x}_x$ is the x-component of the vector $\mathbf{x}$). Vector inequalities apply term by term.

2. Mathematics

We begin by defining the mathematical framework for the analysis of frictionless grasping in the plane. It is convenient to define several coordinate frames and represent them as 3×3 homogeneous transformation matrices (Paul 1981). Let $\mathbf{C}_i$ be the contact frame associated with the ith contact point (see Fig. 1). Then

$$\mathbf{C}_i = \begin{bmatrix} \hat{\mathbf{n}}_{C_i} & \hat{\mathbf{o}}_{C_i} & \mathbf{p}_{C_i} \\ 0 & 0 & \end{bmatrix}, \qquad i = \qquad n_c, \quad (1)$$

where $\hat{\mathbf{o}}_{C_i}$ is the ith contact normal directed inwardly with respect to the object, $\hat{\mathbf{n}}_{C_i}$ is the contact tangent, $\mathbf{p}_{C_i}$ is the position of the contact, and n_c is the number of contact points. There are n_b body frames, $\mathbf{B}_i$,

$$\mathbf{B}_i = \begin{bmatrix} \hat{\mathbf{n}}_{\mathbf{B}_i} & \hat{\mathbf{o}}_{\mathbf{B}_i} & \mathbf{p}_{\mathbf{B}_i} \\ 0 & 0 & \end{bmatrix} \qquad i = \qquad , n_b, \quad (2)$$

that are fixed to the ith body, with its origin $\mathbf{p}_{\mathbf{B}_i}$, at the center of mass. At the base joint of the ith finger, we define

$$\mathbf{T}_i = \begin{bmatrix} \hat{\mathbf{n}}_i & \hat{\mathbf{o}}_i & \mathbf{p}_i \\ 0 & 0 & 1 \end{bmatrix} \qquad = \qquad , n_f, \quad (3)$$

where n_f is the number of fingers. The frames' origins are at the centers of the joints about which the actuators apply torques τ_i, $i = 1, \ldots, n_f$.

Velocity Constraints

If there were no contacts between any of the bodies, then the hand and object would be free to move in any manner. However, when executing a grasp, the contacts constrain their motion. Consider two rigid

Fig. 2. A pair of rigid bodies in point contact.

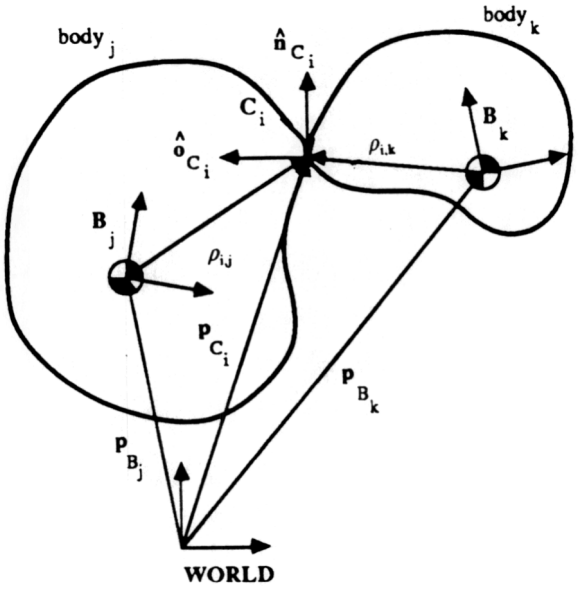

bodies in contact at the point $\mathbf{p}_{C_i}$, as shown in Figure 2. Let $\mathbf{p}_{i,j}$ be the ith contact point on the jth body. The velocity of that contact point on the jth body is

$$\dot{\mathbf{p}}_{i,j} = \dot{\mathbf{p}}_{\mathbf{B}j} + \omega_{\mathbf{B}j} \times \rho_{i,j} \tag{4}$$

where $\dot{\mathbf{p}}_{\mathbf{B}_j}$ is the velocity of the center of gravity of the jth body, $\rho_{i,j}$ is the position of the ith contact point with respect to the jth body, and $\omega_{\mathbf{B}_j}$ is the angular velocity of the jth body. Writing equation (4) in matrix form saving only those components relevant to the two-dimensional problem yields

$$\dot{\mathbf{p}}_{i,j} = \begin{bmatrix} 0 & (-\rho_{i,j})_y \\ 0 & 1 \quad (\rho_{i,j})_x \end{bmatrix} \begin{bmatrix} \dot{\mathbf{p}}_{\mathbf{B}_j} \\ |\omega_{\mathbf{B}_j}| \end{bmatrix}, \tag{5}$$

where $|\omega_{\mathbf{B}_j}|$ is the magnitude of $\omega_{\mathbf{B}_j}$. The relative velocity at the contact point is

$$\mathbf{v}_i = \dot{\mathbf{p}}_{i,j} - \dot{\mathbf{p}}_{i,k}. \tag{6}$$

Since the bodies slide or roll on one another or separate, the relative velocity constraint imposed by the contact is given by

$$\hat{\mathbf{o}}_{\mathbf{C}_i} \quad \mathbf{V}_i \geq 0, \tag{7}$$

for which equality is in effect during sliding and rolling, and inequality implies that the objects are separating.

If we consider the two bodies to be pinned together at the ith contact point, as is the case for the palm and a finger, it is only possible for the bodies to rotate about the joint. Thus the relative translational velocity at the joint must be zero:

$$\mathbf{v}_i = \mathbf{0}. \tag{8}$$

Using inequality (7) for each contact point and Eq. (8) for each finger joint, the system's velocity constraints at a given instant may be written as

$$[\mathbf{V}_\theta \quad \mathbf{V}_{ob} \quad \mathbf{V}_p] \begin{bmatrix} \dot{\theta} \\ \dot{\mathbf{q}}_{ob} \\ \dot{\mathbf{q}}_p \end{bmatrix} \geq \mathbf{0}, \tag{9}$$

where $\dot{\theta}$ is the vector of joint velocities, $\dot{\mathbf{q}}_{ob}$ is the velocity of the object, and $\dot{\mathbf{q}}_p$ is the velocity of the palm. The quantity $\mathbf{V}_{ob}\dot{\mathbf{q}}_{ob}$ represents the components of the velocities of the contact points on the object in the directions of their respective contact normals and $\mathbf{V}_\theta\dot{\theta}$ and $\mathbf{V}_p\dot{\mathbf{q}}_p$ represent the velocities for contact points on the fingers and the palm, respectively.

2.2. Static Equilibrium

The hand/object system must satisfy inequality (9) and the equations of static equilibrium. Referring again to Fig. 1, we write

$$\sum_{i=1}^{n_c} \mathbf{f}_i = -m_{ob}\mathbf{g}, \tag{10}$$

$$\sum_{i=1}^{n_c} \mathbf{p}_{C_i} \times \mathbf{f}_i = -m_{ob}\mathbf{p}_{B_i} \times \mathbf{g}, \tag{11}$$

$$\tau_k + \sum_{i \in \Omega_k} -\tau_k(\mathbf{p}_{C_i} \times \mathbf{f}_i)_z = -m_k{}^{\tau_k}(\mathbf{p}_{B_k} \times \mathbf{g})_z \tag{12}$$

$$k = \quad , n_f,$$

where $\Omega_k = \{i |$ the ith contact is on the kth finger$\}$, m_k

is the mass of the kth finger, m_{ob} is the mass of the object, $\mathbf{g}^T = [0 \quad -g \quad 0]$, and g is the gravitational acceleration constant. Equations (10) and (11) are the force and moment balance equations, respectively, for the object. Equation (12) is the moment balance for the kth finger. Writing Eqs. (10)–(12) in matrix form for the two-dimensional problem gives

$$\mathbf{Ax} = \mathbf{b}, \tag{13}$$

where

$$\mathbf{A} = \begin{bmatrix} \mathbf{W}_O & \mathbf{0} \\ \mathbf{W}_F & \mathbf{I} \end{bmatrix}, \quad \mathbf{x} = \begin{bmatrix} \mathbf{c} \\ \boldsymbol{\tau} \end{bmatrix}, \quad \mathbf{b} = \begin{bmatrix} \mathbf{w} \\ \mathbf{s} \end{bmatrix},$$

$\boldsymbol{\tau}$ is the vector of joint moments ($n_f \times 1$), $\mathbf{c}$ is the vector of contact force magnitudes ($n_c \times 1$), $\mathbf{w}$ is the vector of gravity forces and moments acting on the object (3×1), $\mathbf{s}$ is the vector of gravity moments acting about the joint axes ($n_f \times 1$), $\mathbf{I}$ is the identity matrix ($n_f \times n_f$), $\mathbf{0}$ is a zero matrix ($3 \times n_f$), $\mathbf{W}_O$ is the object wrench matrix ($3 \times n_c$) as defined by Salisbury (Mason and Salisbury 1985), and $\mathbf{W}_F$ is the wrench matrix for the fingers ($n_f \times n_c$). The elements of $\mathbf{W}_O$, $\mathbf{w}$, $\mathbf{W}_F$, and $\mathbf{s}$ are defined as follows. The upper left partition of the equilibrium equation (13) is the same as that labeled Eq. 5.2 on page 41 in Mason and Salisbury (1985). It refers only to the object and is defined for the two-dimensional case as

$$\mathbf{W}_O = \begin{bmatrix} \hat{\mathbf{o}}_{C_1} & & \hat{\mathbf{o}}_{C_{n_c}} \\ (\mathbf{p}_{C_1})_x(\hat{\mathbf{o}}_1)_y - (\mathbf{p}_{C_1})_y(\hat{\mathbf{o}}_1)_x & \cdots & (\mathbf{p}_{C_{n_c}})_x(\hat{\mathbf{o}}_{n_c})_y - (\mathbf{p}_{C_{n_c}})_y(\hat{\mathbf{o}}_{n_c})_x \end{bmatrix}. \tag{14}$$

The gravity force and moment acting on the object (with respect to the world coordinate frame) is

$$\mathbf{w} = -m_{ob} \begin{bmatrix} \mathbf{g} \\ (\mathbf{p}_{B_1} \times \mathbf{g})_z \end{bmatrix} \tag{15}$$

The lower partition of $\mathbf{A}$ is the equilibrium equations for the fingers. The finger wrench matrix $\mathbf{W}_F$ is

$$\mathbf{W}_F = \begin{bmatrix} e_{1,1} & e_{1,2} & \cdots & e_{1,n_c} \\ \vdots & \vdots & & \vdots \\ e_{n_f,1} & e_{n_f,2} & \cdots & e_{n_f,n_c} \end{bmatrix}, \tag{16}$$

where

$e_{i,j} = (\mathbf{p}_{C_j})_x(\hat{\mathbf{o}}_j)_y - (\mathbf{p}_{C_j})_y(\hat{\mathbf{o}}_j)_x$ if the jth contact is on the ith finger,

$e_{i,j} = 0$ otherwise, $i = 1, \ldots, n_f$; $j = 1, \ldots, n_c$.

The gravity moments acting on the fingers are given by

$$\mathbf{s} = \begin{bmatrix} s_1 \\ \vdots \\ s_{n_f} \end{bmatrix}, \quad k = \qquad, n_f, \tag{17}$$

where $s_k = -m_k{}^{T_k}(\mathbf{p}_{B_k} \times \mathbf{g})_z$, k is the finger number, and $\mathbf{T}_k$ is the coordinate frame defining the base of the kth finger.

2.3. Object Motion

To plan grasps, we must be able to predict the motion of the object, given the palm and finger motions. If we consider an infinitesimal increment in time, we can rewrite inequalities (9) in terms of differential motions as

$$\mathbf{V}_{ob}\mathbf{dq}_{ob} \geq -[\mathbf{V}_\theta \quad \mathbf{V}_p] \begin{bmatrix} \mathbf{d}\theta \\ \mathbf{dq}_p \end{bmatrix}, \tag{18}$$

where only $\mathbf{dq}_{ob}$ is unknown. Inequality (18) represents the kinematic constraints on the motion of the object. If we solve for $\mathbf{dq}_{ob}$, we find that the solution is not unique. Figure 1 shows an initial grasping configuration. After moving the palm and fingers a small amount, the object will move to a new position. Figure 3 illustrates an ambiguity inherent in the kinematic constraints (18). Both Figures 3a and 3b show kinematically admissible solutions, but the position of the object shown in 3a is physically incorrect if there is no friction present. We can resolve the kinematic ambiguity by noting that if the motions are slow and there is no friction, then the object must move to minimize its potential energy. Thus the motion is given by the solution to the following linear program

Fig. 3. The ambiguity inherent in the kinematic constraints.

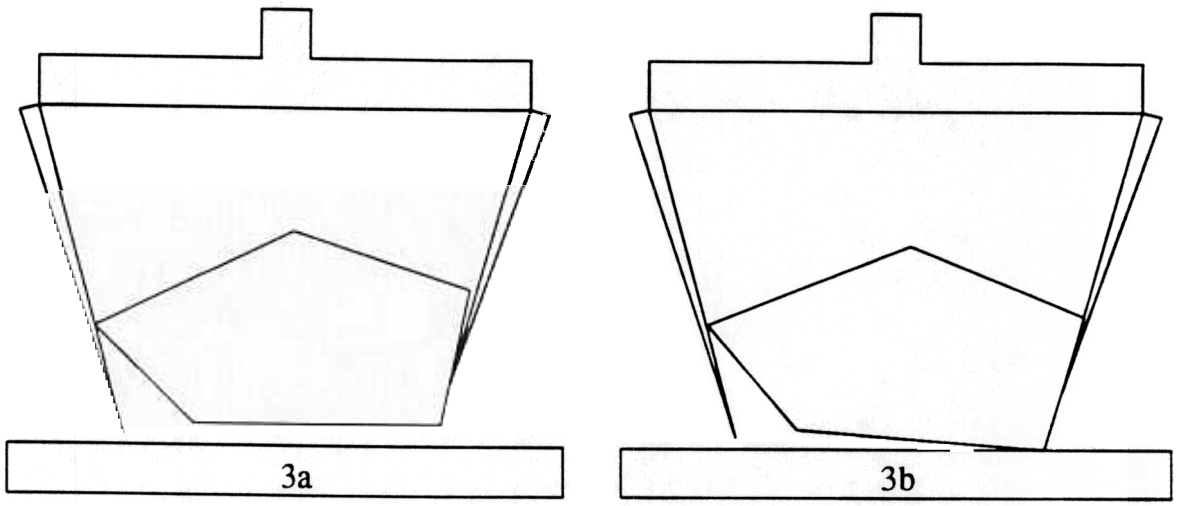

$$\text{Minimize} \quad y = m_{ob}\gamma^T\dot{\mathbf{q}}_{ob}, \tag{19}$$

$$\text{Subject to} \quad \mathbf{V}_{ob}\dot{\mathbf{q}}_{ob} \geq \xi, \tag{20}$$

$$\dot{\mathbf{q}}_{ob} \text{ unrestricted}, \tag{21}$$

where $\gamma = [0 \quad g \quad 0]$ and $\xi = -[\mathbf{V}_\theta \quad \mathbf{V}_p]\begin{bmatrix}\dot{\theta}\\ \dot{\mathbf{q}}_p\end{bmatrix}$. The linear program defined by Eqs. (19)–(21) is the velocity formulation of the object motion. Its physical interpretation is that the object velocity must satisfy the velocity constraints while minimizing the object's rate of potential energy gain. The theory of linear programming provides a dual formulation for every linear program (Gill, Murray, and Wright 1981). The dual of the velocity formulation is the force formulation

$$\text{Maximize} \quad z = \xi^T\lambda, \tag{22}$$

$$\text{Subject to} \quad \mathbf{V}_{ob}^T\lambda = m_{ob}\gamma, \tag{23}$$

$$\lambda \geq \mathbf{0}. \tag{24}$$

The variable λ of the force formulation is the dual variable of the velocity formulation and is the vector of Lagrange multipliers associated with the velocity constraints. They are also known to be the magnitudes of the contact forces (Whittaker 1937), which were denoted earlier as **c**. Note that the objective function of the force formulation is the rate of work done by the object on the hand and that constraints (23) are the equations of equilibrium of the object taken with respect to its center of mass. Thus, the object's motion is determined by minimizing the virtual work performed on the object while maintaining static equilibrium with nonnegative contact forces (constraints (24)).

2.4. Tippability

In order to lift an object that is resting on a flat surface, using smooth fingers, we must first be able to cause the object to tip. After the hand is positioned and the fingers begin to squeeze, the object will either tip toward the palm or not move at all. If the object begins to move, it can do so in only two ways. It may translate, completely breaking contact with the support, or it may rotate so that one end of the support segment maintains contact. Translation occurs under special circumstances with three point contacts and in symmetric cases with only two, but normally the object will break contact with the supporting surface by rotating as shown in Fig. 3B. In either case, if the object moves it possesses an important quality that we call tippability.

Fig. 4. A right tippable initial grasping configuration.

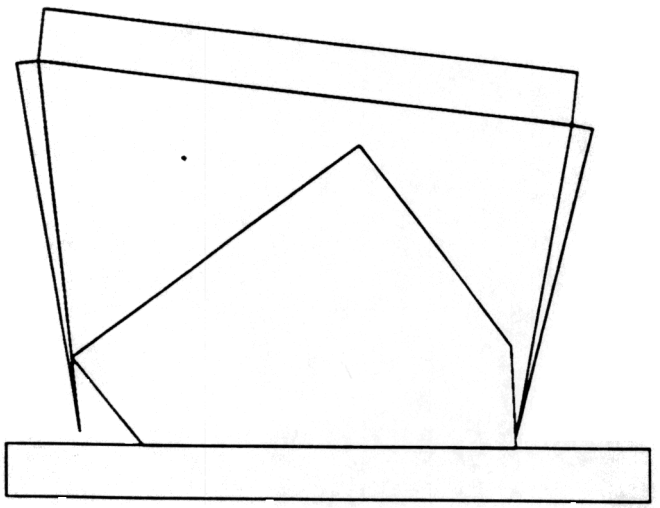

Fig. 5. Determining the edge subregions of the right tippability region.

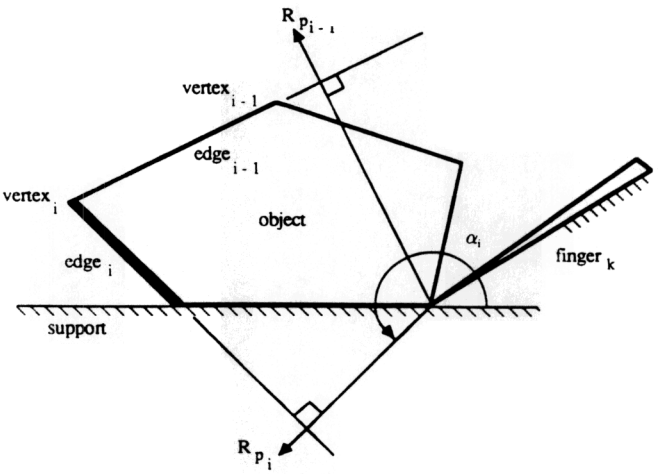

Definition

An object is *tippable* if there exists finger contact positions on its perimeter (excluding the supporting edge) for which increasing the fingers' contact forces drives at least one supporting contact force to zero.

Determining the tippability of an object allows us to place the hand on it with prior knowledge of the instantaneous result of squeezing the fingers together. In order to define tippability, consider a fingertip in contact with the object at the right support contact, as shown in Fig. 4. Note that the contact normal at the fingertip has a negative x-component. We define the right tippability region as that part of the perimeter of the object for which a finite contact force will cause the left support contact force to go to zero. In other words, the moment of the contact force about the right support contact must have the same sense as that generated by the left support contact force. At vertices, we consider all contact normals which could be achieved by an edge of a finger in contact with that vertex. (A contact normal is defined by the object's edge for the case of a finger tip contact and by the finger's edge for the case of a finger contacting a vertex of the object.) Also, since we want to balance the contact force component in the negative x-direction, only those points whose contact normals have a positive x-component are considered. Let the vertices be numbered in increasing order moving counterclockwise around the object and let the ith edge lie between the ith and $(i + 1)$th vertices. The right tippability region is delimited by considering two sets of rays R_{p_i}; $i = 1, \ldots, k$ (see Figure 5) and R_{v_i}; $i = 1, \ldots, k$ (see Figure 6) emanating from the right support contact point. The ray R_{p_i} is perpendicular to the ith edge of the object, and the ray R_{v_i} passes through the ith vertex.

The right tippability region of a k-sided polygon is divided into $2k$ subregions. For each edge of the object, there is an edge subregion which is a portion of the edge. For each vertex, the vertex subregion is a range of finger angles. Since access to the supporting edge and vertices is obstructed by the support, the subregions corresponding to them are empty. Measuring counterclockwise from the x-direction, we define α_i and β_i; $i = 1, \ldots, k$ to be the angles of R_{p_i} and R_{v_i}, respectively. The ith edge subregion is the portion of the ith edge for which the contact normal passes above the right support contact. This is seen to be the part of the ith edge between the ray R_{p_i} and the ith vertex. This subregion is only valid if $\pi/2 < \alpha_i < 3\pi/2$, because of the requirement that the contact normal have a positive x-component. Note that the subregion corresponding to the ith edge, shown bold in Figure 5, is the entire edge, but that the subregions for all of the other edges are empty. The ith vertex subregion, shown as a bold arc in Figure 6, is the set of finger angles, ϕ_i, for which the contact normals have a positive x-component and pass above the right support

Fig. 6. Determining the vertex subregions of the right tippability region.

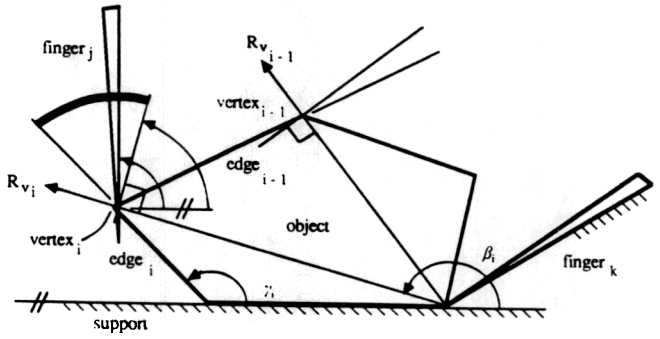

Fig. 7. A form-closure grasp of the object.

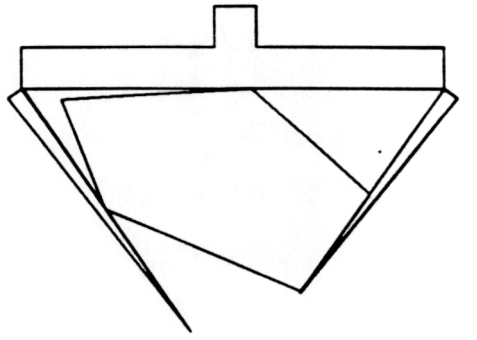

11

contact. The subregion is defined as $\{\phi_i | \beta_i - \pi/2 < \phi_i \gamma_i\}$, where $\beta_i - \pi/2$ is the angle of the perpendicular to the ray R_{v_i} and $\gamma_i = \text{atan } 2\ (y_i - y_{i+1}, x_i - x_{i+1})$, where atan 2 is the inverse tangent function, which computes angles from $-\pi$ to π, and x_i and y_i are the x- and y-positions of the ith vertex. The condition $0 < \gamma_i < \pi$ is to ensure that the x-component of the contact normal is positive. Also, the ith vertex subregion is empty if $\gamma_i < \beta_i - \pi/2$, which will occur when the ith edge subregion is empty. The vertex subregion for the ith vertex is shown as a heavy arc in Fig. 6. Note that all the other vertex subregions are empty, since $\beta_k - \pi/2 > \gamma_k$, $k \neq i$. The left tippability region may be obtained in a similar way.

If the tippability regions for a convex polygon are empty, then we are guaranteed that the object cannot be lifted in a quasi-static mode without friction. This condition will occur when there is no point on the exposed perimeter of the object that has a contact normal that passes through the support outside the supporting edge of the object. As a result, any moment applied to the object by a frictionless contact will be resisted by the supporting contact forces.

Tippability analysis is similar to work done by Mason (Mason and Salisbury 1985) and Brost (1985), who determined the qualitative motion of the object based on the motion and position of the fingers' contact points. We were able to exactly predict the velocity of the object via the object motion linear program (19–21). This was possible because we had precise knowledge of the external force acting on the object. Mason and Brost were not able to do so, because the force acting between the object and the supporting plane was dependent upon unknown surface variations.

2.5. Grasp Stability

A frictionless grasp begins as shown in Fig. 1, with the object on its support and the hand just touching it. Our goal is to achieve an enveloping grasp of the object. An enveloping grasp is characterized by the object's being completely restrained with respect to the hand when the finger joints are locked. This type of grasp has been termed a *form-closure* grasp (see Fig. 7) by Lakshminarayana (1978). Form closure requires the satisfaction of two conditions. First, the kinematic constraints (18) must be satisfied, which disallows mutual penetration of the hand and the object. Second, no nontrivial motion of the object may satisfy the kinematic constraints when the palm and fingers are fixed (*i.e.*, $d\mathbf{q}_p = 0$, $d\theta = 0$). In other words, the conditions for form closure are that the matrix V_{ob} must be such that the system of inequalities

$$\mathbf{V}_{ob}\mathbf{dq}_{ob} \geq \mathbf{0}$$

admits only the trivial solution, $d\mathbf{q}_{ob} \equiv \mathbf{0}$.

Form closure is equivalent to requiring that the contact forces may be combined to resist any applied force and moment. This condition guarantees that the object can always be held in equilibrium. The partition of equation (13), which represents the equilibrium of the object is

$$\mathbf{W}_O\mathbf{c} = \mathbf{w}'$$

where $\mathbf{w}'$ may be any disturbing force. Also, the contact forces must be compressive, not tensile, so

$$\mathbf{c} \geq \mathbf{0}. \tag{27}$$

Since $\mathbf{w}'$ is completely free, Eqs. (26) and (27) imply that any vector in Euclidean 3-space, R^3, can be represented by a nonnegative linear combination of the columns of $\mathbf{W}_O$. In other words, the nonnegative column span of $\mathbf{W}_O$ must be equivalent to R^3. This is why at least four contact points are needed for a form-closure grasp (see Trinkle 1985, Appendix A, pp. 29, 30 for a proof).

Let $\mathbf{y}_i$, $i = 1, \ldots, n_c$, be the columns of $\mathbf{W}_O$. The nonnegative span of $\mathbf{y}_i$ is given by $C^+ = \{\mathbf{u} | \mathbf{u} = \sum_{i=1}^{n_c} \alpha_i \mathbf{y}_i;\ \alpha_i \geq 0 \text{ for all } i\}$. Between the initial state (Fig. 1) and the first time that the object is in a form-closure grasp, the object is, in general, in equilibrium through *force closure* (Reuleaux 1963). A force-closure grasp occurs when $C^+ \subset R^3$ and $\mathbf{w}' \in C^+$. In other words, the object is in equilibrium because the gravity force holds it against the contact points (see Fig. 8). If gravity were acting in the opposite direction, then the object would be unstable. In some cases $\mathbf{w}' \notin C^+$, so the object becomes unstable and falls until a new set of contacts gives rise to a new C^+ that contains $\mathbf{w}'$. This condition usually arises when the object has three contacts and one of the contact forces goes to zero during manipulation.

Fig. 8. A typical force-closure grasp.

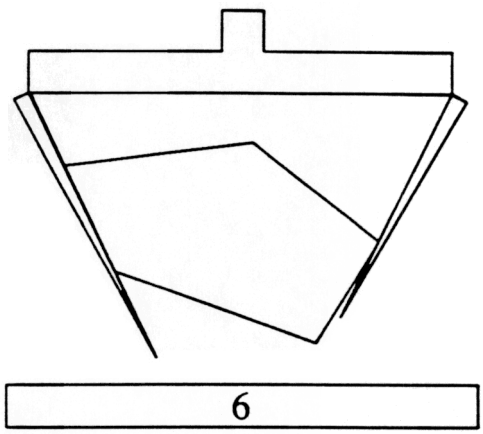

3. The Planner/Simulator

The mathematics given above in Section 2 have been used to develop a planner/simulator for generating enveloping grasps in the plane. The flow chart (see Figure 9) shows the input to be the kinematic, geometric, and other physical data of the hand, object, and support. After reading the data, all of the coordinate transforms are initialized. Next the left and right tippability regions of the object are computed. If the regions are empty, then the object cannot be lifted and the program exits. If the object is tippable, then the planner attempts to find an initial grasping configuration in one of the tippability regions. If due to hand kinematics, a grasping configuration cannot be found, then an alternative scheme must be used to place the hand. For each placement, tippability must be checked. If a tipping configuration cannot be found for any placement, the program exits.

If an initial configuration for the hand is found from which the object can be tipped, the planner determines displacement increments for the hand: palm position and orientation changes and finger angle increments. These increments are sent to the simulation module, which computes the resulting motion of the object. The configuration of the hand and object are then updated and sent to the planner for it to plan the next increments. When the planner determines that a suitable grasp has been achieved, it outputs the trajectory and stops.

3.1. The Simulator

The simulator that we have developed is specific to two-dimensional, frictionless grasping. Where possible, we have relieved the simulator of some of the computational burden that would be required for a completely general simulator.

As stated, only line segment and point contacts may occur among the bodies represented in our system. We also have argued that a line segment contact may be treated as a pair of point contacts, one at each end of the segment. The simulator must locate and keep

Fig. 9. Flowchart for planner/simulator.

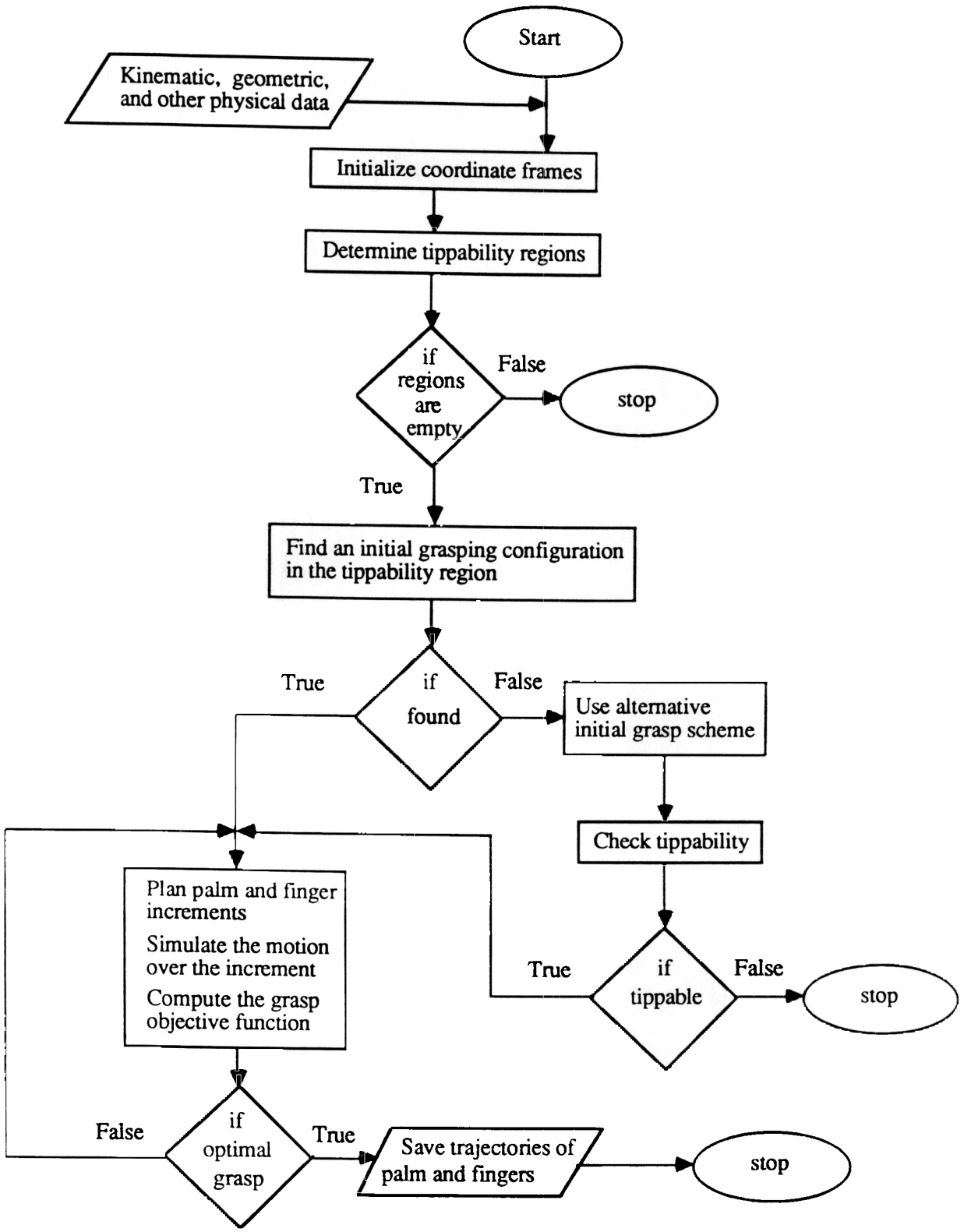

Fig. 10. The palm edges of the hand are drawn heavy.

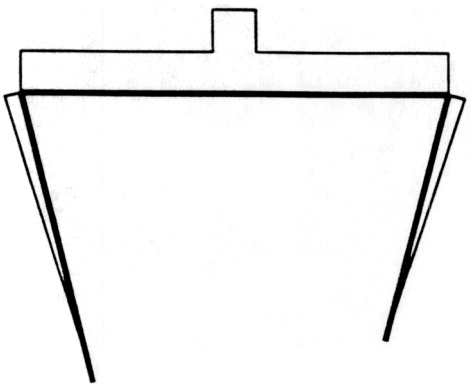

track of the contact points while manipulating the object to create a form closure grasp. To make this as simple as possible, we use the fact that we are only looking for enveloping grasps. In an enveloping grasp, the object may only contact the hand on the "palmar edges," by which is meant those line segments shown bold in Figure 10. When looking for contacts, we need only consider the palmar edges, the support line, $y = 0$, and all of the edges of the object.

After moving the hand, we must minimize the object's potential energy while preventing interference between the object and the other bodies. Attempting to find the position and orientation of the object by solving a nonsmooth optimization (Lemarechal and Mifflin 1977) problem is difficult and prone to error. Given the positions of the palm and fingers, the objective function is linear, but the constraints are nonlinear, nonsmooth inequalities which represent the interiors of the bodies as functions of the object's position and orientation. The rotations of the object give rise to trigonometric terms, and its vertices are responsible for discontinuities in the constraint derivatives.

As an alternative to this formulation, we chose to use an active set method. The method consists of three steps. First the force formulation of the velocity problem, Eqs. (22)–(24), is solved to determine the set of contacts that will be active at the beginning of the current increment in the motion of the hand. This active set, which corresponds to nonzero values of the Lagrange multipliers, is used to generate a system of *smooth*, nonlinear, algebraic constraint *equations* (not inequalities),[2]

$$c_i(\mathbf{q}_{ob}) = 0, \qquad i = 1, \ldots, n_c, \tag{28}$$

that we assume are in effect throughout the entire motion increment. The second step is the simultaneous solution of the constraint equations, the result of which is the new position and orientation of the object. The third step is a consistency check. We assumed in the first step that the active contact set is active for the entire motion increment and that no changes in the contact conditions are encountered. It is clear that this is not always the case, so we must check for changes. One way that a change can occur is by a collision between two bodies. Another way is by an edge contact's changing to a tip contact, or vice versa. This change occurs when a vertex of the object that had been in contact with a finger edge slides past the tip during the motion increment or when a contacting fingertip slides past a vertex, which then remains in contact with the finger's edge. The last way in which the contact conditions can change is by one of the contact forces going to zero, resulting in a lost contact. If any of these conditions are found, the increment is adjusted; the motion is computed up to the point of the change in contact conditions; contact conditions are updated, and the new configuration is sent back to the planner. The object motion is not integrated over the original increment.

During an increment in the simulation of the motion, we have assumed that certain contacts are maintained. This assumption enabled us to write the active constraints as a system of equalities in terms of the position and orientation of the object $\mathbf{q}_{ob}$. Figure 11 illustrates the two possible types of contacts; they are both vertex-to-edge contacts, but result in very different constraint equation forms because of their relationship to the object's frame. Figure 11A shows an edge contact (an edge of a finger contacts a vertex of the object). An edge contact is characterized by the fact that the contact point on the object is fixed with respect to the object's frame, whereas the contact point on the finger moves with respect to its coordinate frame. The other type of contact is a tip contact (see Figure 11B.). In this case, the contact moves with respect to the object, but not with respect to the finger.

The computation required for each increment of motion in the simulation is: 1) the solution of a linear program with three independent variables, 2) the solu-

2. See Appendix for the derivation of the contact constraints.

Fig. 11. Contact types. A. Edge contact. B. Tip contact.

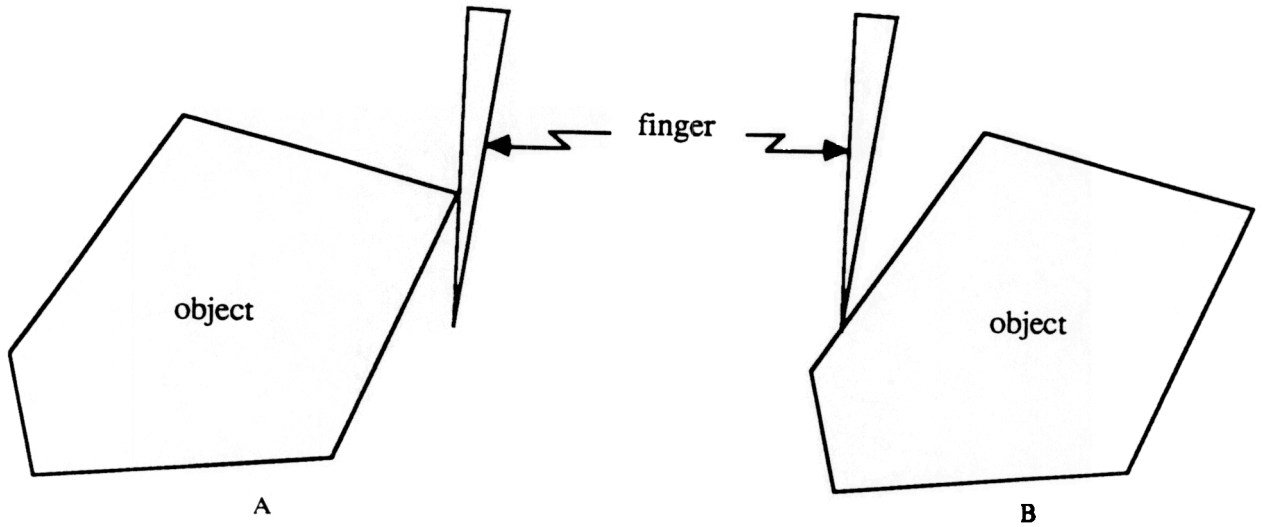

tion of a system of three nonlinear algebraic equations, and 3) a search for new contact conditions. If a new contact arises during the increment, then the results of item 2) above are discarded, the increment is shortened, 2) is repeated, and the contact set is adjusted to include the new condition detected in 3).

3.2. The Planner

Planning is partitioned into three phases. The first phase is the *pre-liftoff* phase, during which the hand is placed in a suitable position for grasping. Before positioning the hand, the planner computes the tippability regions of the object. If they are empty, then no plans are made because the object cannot be picked up. If the tippability regions are not empty, then the planner attempts to find an initial grasping configuration consistent with the tippability regions. If the hand can be placed on the object with one fingertip at a support contact and the other finger within the appropriate tippability region, then squeezing the fingers will tip the object, moving it toward the palm (see Fig. 4). On the other hand, if the kinematics of the hand preclude all grasps within the tippability regions, then the hand is centered over the object and closed until the fingers touch the object. Since the resulting initial grasping configuration is not in either the left or right tippability region, we must determine whether squeezing will tip the object by solving the velocity formulation of the object motion problem, Eqs. (19)–(21). If there is a feasible solution, then the object will tip, and the vanishing of dual variable(s) will indicate which support contact(s) is (are) broken at the onset of motion. We call such an initial grasping configuration tippable.

One aspect of pre-liftoff planning that we will not discuss is the computation of a trajectory that can be used to move the hand to the initial grasping configuration. We do not address that issue here, but refer the reader to a paper by Kuan, Zamiska, and Brooks (1985).

The second phase of planning is called the *lifting* phase. It is characterized by independence in the planner's choice of the finger angle increments. It begins when the object first starts to move, and ends when a form-closure grasp is achieved. During the lifting phase, the grasp plan is generated incrementally. The planner chooses small finger angle increments that will cause the object to move toward the palm, sends the proposal to the simulator, and waits for the results of the simulation before planning the next increment. Thus the planner always uses the most up-to-date information available about the state of the system to plan the motion of the hand. Also, the planner does not know whether the object will be dropped. It only knows what will happen the instant that the proposed motion starts. It does not have knowledge about finite

Fig. 12. The width of the object.

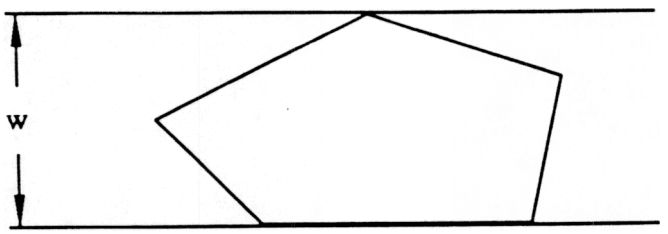

manipulations. However, if we define the width w of the object as the minimum distance between all possible pairs of parallel lines containing the object (see Fig. 12) and the distance between the fingertips as d, and if we know that the object is in the hand and that $d < w$ for the duration of a finite manipulation, then the object cannot be dropped (Toussaint 1984).

The lifting phase ends and the *grip adjustment* phase begins when a form closure grasp is achieved. Form closure is signaled by the infeasibility of the velocity linear program, equations (19)–(21). Since our goal is to determine an appropriate form closure grasp, the object is manipulated in a way which maintains form closure. Thus there must be four contact points, yielding four constraint equations (28). Since there are five parameters which specify the configuration of the hand, there is only one independent variable with which the object may be manipulated. Therefore, the planner chooses the angle increment for the first finger and computes the increments for the palm and the second finger.

Once the object is in a form closure grasp, the arm can move while the object remains at rest relative to the hand. During the motion, the object and the fingers will be subject to external disturbing forces $\mathbf{w}'$ and $\mathbf{s}'$, respectively, caused by gravity and the acceleration of the hand. The disturbing force will give rise to contact forces and moments that restrain the object, maintaining the equilibrium of the hand/object system. The solution of the equilibrium equation (13) gives the values of the contact force magnitudes and joint torques. Since $\mathbf{A}$ is generally rectangular, the solution to Eq. (13) is given as (Greyville 1959)

$$\mathbf{x} = \mathbf{r} + \mathbf{N}_A\mathbf{k}, \tag{29}$$

where $\mathbf{r} = \mathbf{A}\dagger\mathbf{b}$, $\mathbf{k}$ is an arbitrary vector, and $\mathbf{N}_A$ is a matrix whose columns form a basis for the null space of $\mathbf{A}$. Partitioning Eq. (29) into torques and contact force magnitudes, we write

$$\begin{bmatrix}\mathbf{c}\\ \tau\end{bmatrix} = \begin{bmatrix}\mathbf{d}\\ \mathbf{e}\end{bmatrix} + \begin{bmatrix}\mathbf{H}\\ \mathbf{Q}\end{bmatrix}\mathbf{k}.$$

In our assumptions, we stated that the fingers moved under exact position control. Thus if $\mathbf{w}' = \mathbf{0}$ and $\mathbf{s}' = \mathbf{0}$, then $\mathbf{c} = \mathbf{0}$ and $\tau = \mathbf{0}$; that is, there is no internal grasp force, no preload. Also, for a form-closure grasp, increasing one of the contact forces causes all of the others to increase. Thus positioning the fingers exactly implies that the sum of the magnitudes of the contact forces acting on the object will be a minimum. This condition can be stated mathematically as

$$\text{Minimize} \quad y = \mathbf{1}^{\mathrm{T}}\mathbf{c}, \tag{31}$$

$$\text{Subject to} \quad \mathbf{c} \geq \mathbf{0},$$

where $\mathbf{1}$ is a vector with all of its elements equal to 1. Using Eq. (30), we obtain a linear program in the variable $\mathbf{k}$:

$$\text{Minimize} \quad y = \mathbf{1}^{\mathrm{T}}(\mathbf{d} + \mathbf{H}\mathbf{k}), \tag{33}$$

$$\text{Subject to} \quad \mathbf{H}\mathbf{k} \geq -\mathbf{d},$$

$$\mathbf{Q}\mathbf{k} \geq -\mathbf{e} + \tau_{\min},$$

$$-\mathbf{Q}\mathbf{k} \geq \mathbf{e} - \tau_{\max}$$

The linear program requires that the contact force magnitudes be greater than or equal to zero (inequality (34)) and that the actuator torques do not exceed their limits (inequalities (35) and (36)).

Denote the minimum objective function value by y^*. The planner uses y^* as the objective value to drive grip adjustment. Since there is only one independent variable, say θ_1 for argument's sake, the grip is adjusted by numerically determining the gradient of y^*. The current position of the first finger, $\theta_1^{(k)}$, is adjusted to its next value, $\theta_1^{(k+1)}$, as follows:

$$\theta^{(k+1)} = \theta^{(k)} - \alpha\frac{y^*(\theta_1^{(k)} + \epsilon) - y^*(\theta_1^{(k)})}{\epsilon} \tag{37}$$

Fig. 13. Achieving an enveloping grasp.

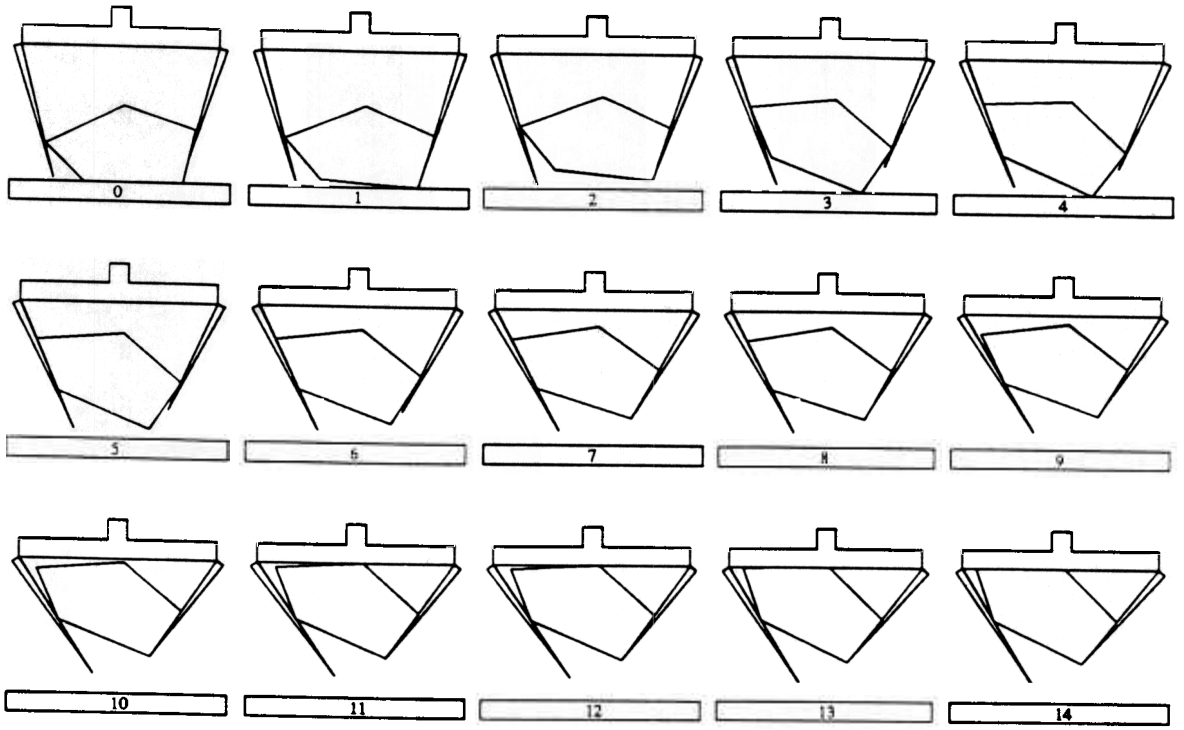

where ϵ is a suitably small change in θ_1 and $\alpha > 0$. Once the new value of θ_1 is chosen, the other finger angle and the position of the object are computed by solving the system of constraint equations (28). When a local minimum of y^* is reached, the grip adjustment phase ends and the plan is complete.

4. Results

The planner/simulator discussed above has been implemented in Fortran 77 using International Mathematics and Statistics Library routines for the solution of systems of nonlinear equations, the solution of linear programs, and the inversion of general matrices. Figure 13 shows a sequence of 15 frames of a grasp which was computed on a Vax 11/750 in 0.153 seconds of cpu time. The important dimensionless parameters of some of the bodies relative to the palm's width were the length of finger 1 = 0.6, the length of finger 2 = 0.7, and the width of the object = 0.4. The masses of the fingers and the object were proportional to their respective areas, and the joint torque limits were chosen to ensure that they would not limit the hand's ability to pick up the object. Planning for this grasp was very simple. In the pre-liftoff phase, the palm was centered over the object, parallel to the support, just high enough so that the longer finger could not touch the support. Then the palm position was fixed for the rest of the grasping sequence. The pre-liftoff phase ended as the fingers were brought into contact with the object. The lifting phase proceeded by moving the fingers together at equal angular rates, continuing until a form-closure grasp was achieved at frame 11. Note that during the grasping manipulation, the object moves toward the palm in several different three-contact, force-closure grasps. Transitions between the grasps occur when a fourth contact becomes active, forcing one of the previously active contacts to break (see Fig. 13, frames 3,4,5). Once, the force-closure grasp became unstable, because one of the contact forces went to zero. In this case, the object executed a constrained fall until another contact stabilized the grasp again (see Fig. 13, frames 2,3,4). Frames

Fig. 14. The grip adjustment objective as a function of the angle of finger 1 and the choice of the contact to break. The frame numbers are indicated by squares on the right branch. Each branch is caused by manipulating the object to break one contact and maintain the other four. The circled number beside each branch indicates the lost contact leading to the branch.

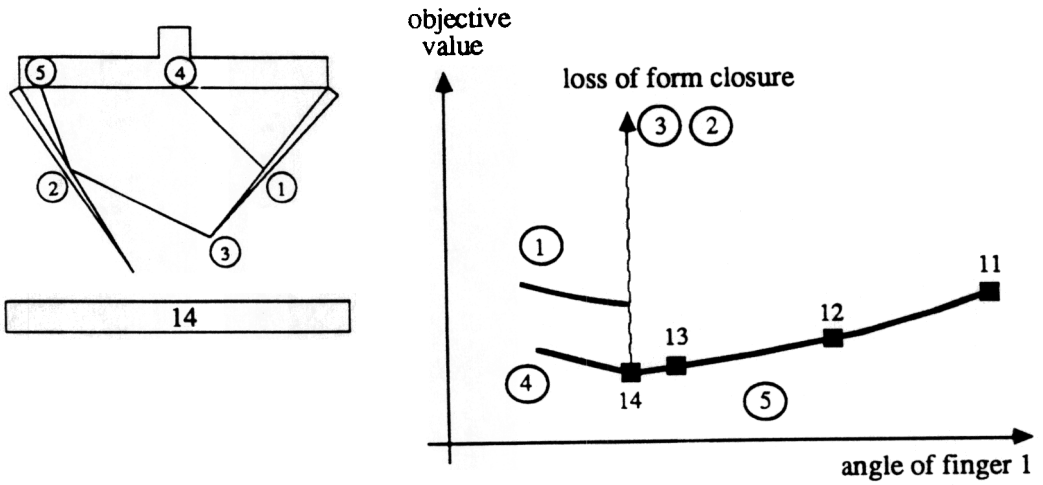

12 to 14 were generated in the grip adjustment phase using the gravity load as the disturbing force $\mathbf{w}'$.

The grasp plan for the hand and object shown in Fig. 13 is accurate for the frictionless case. It can be determined geometrically that the object will rise when squeezed (for any of the configurations shown) if the coefficient of friction is less than 0.35. However, it is important to note that the object will not necessarily follow the same trajectory during the lifting phase, because the object motion linear program neglects friction. If the coefficient of friction is greater than 0.35, then the hand/object mechanism will jam in frame 0, making it impossible to lift the object in the manner shown.

The final grasp, shown in frame 14, has five contact points that cause a discontinuous branch point in the objective y^*. The branches occur because only four contact points can be maintained while manipulating the grasp, but five possible sets of four contacts exist. Two of the five sets do not maintain form closure, so they are not considered for further grip adjustments. Figure 14 shows the grip adjustment objective function in the neighborhood of frame 14. The square on the far right corresponds to frame 11. Moving to the left, the objective value decreases until the object gains the fifth contact point, frame 14. To continue manipulating the grip, one of the contacts must be chosen as the one to break, and the finger motions must be computed to be consistent with maintaining the other four contacts. If either contact 2 or 3 is broken, the grasp loses form closure. This is fairly obvious for 2, since it corresponds to removing the second finger. In the case of the 3rd contact, form closure is lost since the object may rotate counterclockwise about the intersection of the 1st and 4th contact normals, losing contact at points 2 and 5. If contact 1 is broken, the objective value jumps because one of the palm contact forces (which was previously zero) becomes nonzero, effectively adding to the gravity load which must be absorbed by the two contacts on the fingers. Breaking the 5th contact, the object moves back to a previous grasping configuration. Removing the 4th contact is the only possibility for improving the grasp. However, it is found that the grip objective increases for the manipulation that breaks that contact, so frame 14 is the (locally) optimal solution.

5. Conclusion

A system has been developed that can be used to plan (in an off-line mode) and simulate the grasping of convex polygons when friction and dynamic effects are negligible. In the simulation, the grasps are executed under position control with no need for force control or tactile sensing. However, we have assumed that accurate descriptions of the important physical parameters of the bodies are available to the system.

Fig. 15. An edge contact.

The mathematics of frictionless grasping is more general than the software implementation described here. Three-dimensional, nonpolyhedral, nonconvex bodies may be used as well as multilink fingers. The cost of generality is added computational complexity, because collisions become more difficult to detect and the constraint equations are more difficult to solve. In addition, the representation of bodies becomes more complex.

This research is currently being extended to include the effects of friction and uncertainty in geometric knowledge on the motion of the object and grasp planning.

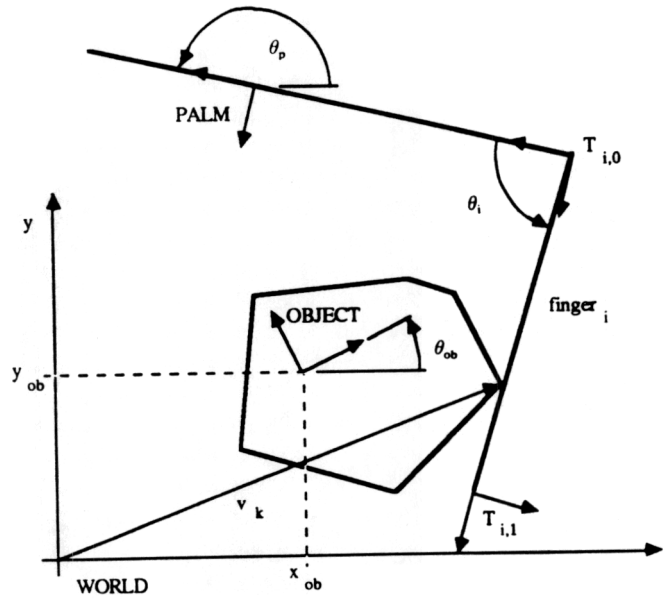

Edge Contact

Figure 15 shows an edge contact on the kth vertex of the object on the ith finger. By edge contact we mean that the edge of the finger contacts a vertex on the object, rather than a line segment on the object. Given that the contact is active, the kth vertex must remain on the line defined by the finger's joint and tip. The equation of a line, l, in the plane $z = 0$, through two distinct points, (x_a, y_a) and (x_b, y_b) can be written as

$$l = -x\,\delta y + y\,\delta x + x_a\,\delta y - y_a\,\delta x = 0. \quad \text{(A.1)}$$

where $\delta x = x_a - x_b$ and $\delta y = y_a - y_b$. The position of the palm is given by x_p, y_p, and θ_p and the transformation matrix relating the *PALM* coordinate frame to the world coordinate frame is

$$PALM = \begin{matrix} \cos\theta_p & -\sin\theta_p & x_p \\ \sin\theta_p & \cos\theta_p & y_p \\ 0 & 0 & 1 \end{matrix} \quad \text{(A.2)}$$

Similarly, the positions of the object and the fingers' joints and tips can be related to the *world* coordinate frame through the following transformations matrices.

Acknowledgments

The authors would like to extend thanks to Professor M. Mintz for his invaluable suggestions.

6. Appendix

The active contact constraint equations are derived here and manipulated into a common form (MACSYMA, Version 10, of M.I.T. and Symbolics, Inc., 1983, was used to perform some of the algebraic manipulations and the trigonometric simplifications of the constraint equations). This form facilitated the writing of a subroutine to compute the constraint values for any number and type of constraints, thereby eliminating the need for different subroutines to handle different numbers and types of constraints.

The active contact set determines a system of nonlinear constraint equations that are functions of the position and orientation of the object. Because the bodies are polygonal, a contact point always involves an edge of one body and a vertex of another (we exclude contacts between vertices because they are unrealizable).

$$\text{OBJECT} = \mathbf{B}_5 = \begin{bmatrix} \cos\theta_{ob} & -\sin\theta_{ob} & x_{ob} \\ \sin\theta_{ob} & \cos\theta_{ob} & y_{ob} \\ 0 & 0 & 1 \end{bmatrix}, \quad \text{(A.3)}$$

$$T_i = \begin{bmatrix} \cos\theta_p & -\sin\theta_p & x_b \\ \sin\theta_p & \cos\theta_p & y_a \\ 0 & 0 & 1 \end{bmatrix},$$

$$T_{i,1} = \begin{bmatrix} \cos(\theta_p + \theta_i) & -\sin(\theta_p + \theta_i) & x_b \\ \sin(\theta_p + \theta_i) & \cos(\theta_p + \theta_i) & y_b \\ 0 & 0 & 1 \end{bmatrix}, \quad \text{(A.4)}$$

$$i = 1, \ldots, n_f.$$

The orientation of the line along the finger is given by the first column in the matrix $T_{i,1}$. Thus the following proportionalities are used to determine the line l:

$$\delta x \propto \cos(\theta_p + \theta_i), \qquad \delta y \propto \sin(\theta_p + \theta_i). \quad \text{(A.5)}$$

The position of the kth vertex of the object with respect to OBJECT is constant and defined in homogeneous form as

$${}^{ob}\mathbf{v}_k = \begin{bmatrix} a_k \\ b_k \\ 1 \end{bmatrix} \quad \text{(A.6)}$$

The position of the vertex in the world is a function of the position of the object and is given by

$$\begin{bmatrix} x \\ y \\ 1 \end{bmatrix} = \text{OBJECT}\ {}^{ob}\mathbf{v}_k = \begin{bmatrix} a_k \cos\theta_{ob} - b_k \sin\theta_{ob} + x_{ob} \\ a_k \sin\theta_{ob} + b_k \cos\theta_{ob} + y_{ob} \\ 1 \end{bmatrix} \quad \text{(A.7)}$$

Substituting x, y, δx, and δy into Eq. (A.1) gives the edge contact constraint as a function of the object's position and the joint angle of the contacting finger.

$$\begin{aligned} l(x_{ob}, y_{ob}, \theta_{ob}, \theta_i) = &-a_k \sin(\theta_p + \theta_i - \theta_{ob}) \\ &+ b_k \cos(\theta_p + \theta_i - \theta_{ob}) \\ &- x_{ob} \sin(\theta_p + \theta_i) \\ &+ y_{ob} \cos(\theta_p + \theta_i) \\ &+ x_a \sin(\theta_p + \theta_i) \\ &- y_a \cos(\theta_p + \theta_i), \\ i = 1, &\ldots, n_f. \end{aligned} \quad \text{(A.8)}$$

In simulating a grasp, the positions of the palm and the fingers are specified. Thus they are known and do not appear as variables in the constraint equations. They are implicit in x_a and x_b.

If the contact is on the palm rather than a finger, then

$$\begin{bmatrix} \delta x \\ \delta y \end{bmatrix} = \begin{bmatrix} \cos\theta_p \\ \sin\theta_p \end{bmatrix}. \quad \text{(A.9)}$$

Choosing x_a and y_a to be one of the fingers' joints and substituting into Eq. (A.1), we get

$$\begin{aligned} l(x_{ob}, y_{ob}, \theta_{ob}) = &(b\delta y + a\delta x)\sin\theta_{ob} \\ &+ (b\delta x - a\delta y)\cos\theta_{ob} \\ &- \delta y x_{ob} + \delta x y_{ob} + x_a \delta y \\ &- y_a \delta x = 0. \end{aligned} \quad \text{(A.10)}$$

If contact is on the support, then

$$\begin{bmatrix} \delta x \\ \delta y \end{bmatrix} = \begin{bmatrix} 1 \\ 0 \end{bmatrix} \quad \text{and} \quad \begin{bmatrix} x_a \\ y_a \end{bmatrix} = \begin{bmatrix} 0 \\ 0 \end{bmatrix}. \quad \text{(A.11)}$$

Thus the constraint for support edge contact is

$$\begin{aligned} l(x_{ob}, y_{ob}, \theta_{ob}) = &a \sin\theta_{ob} + b \cos\theta_{ob} \\ &- y_{ob} = 0. \end{aligned} \quad \text{(A.12)}$$

Tip Contact

For a tip contact, the line l is defined by the position of the kth and the $(k+1)$th vertices (see Fig. 16). Thus

$$\begin{bmatrix} \delta x \\ \delta y \end{bmatrix} = \begin{bmatrix} (a_k - a_{k+1})\cos\theta_{ob} \\ (b_k - b_{k+1})\sin\theta_{ob} \end{bmatrix} \quad \text{(A.13)}$$

The fingertip must lie on l. Therefore $x = x_b$ and $y = y_b$ must satisfy Eq. (A.1). Treating the angle of the ith finger θ_i as an unknown, the position of the fingertip is

$$\begin{bmatrix} x_b(\theta_i) \\ y_b(\theta_i) \end{bmatrix} = \begin{bmatrix} x_a + d_i \cos(\theta_p + \theta_i) \\ y_a + d_i \sin(\theta_p + \theta_i) \end{bmatrix}, \quad \text{(A.14)}$$

Fig. 16. Schematic of a tip contact with the ith finger.

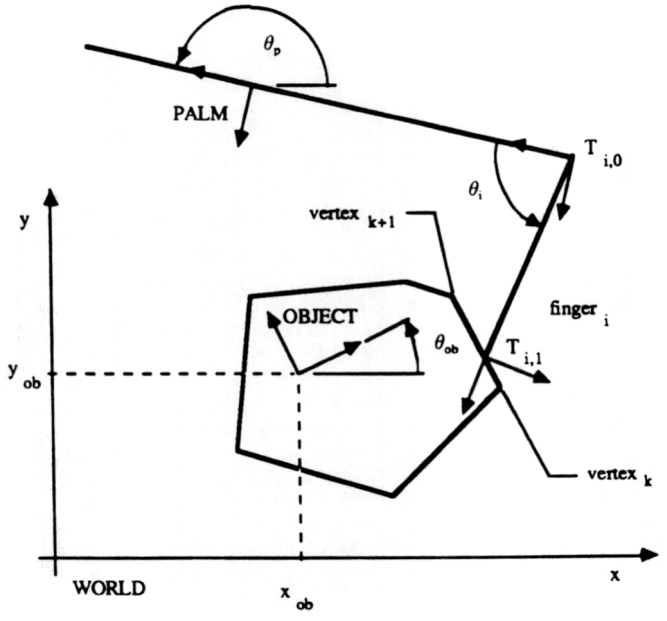

where d_i is the distance between the finger's tip and joint. Substituting Eqs. (A.13) and (A.14) into Eq. (A.1), we obtain the constraint for tip contact:

$$\begin{aligned} l(x_{ob}, y_{ob}, \theta_{ob}, \theta_i) = {} & [-y_a(b_k - b_{k+1}) - x_a(a_k - a_{k+1})]\sin\theta_{ob} \\ & + [y_a(a_k - a_{k+1}) - x_a(b_k - b_{k+1})]\cos\theta_{ob} \\ & + d_i(a_k - a_{k+1})\sin(\theta_p + \theta_i - \theta_{ob}) \\ & - d_i(b_k - b_{k+1})\cos(\theta_p + \theta_i - \theta_{ob}) \\ & + (b_k - b_{k+1})y_{ob}\sin\theta_{ob} \\ & + (a_k - a_{k+1})x_{ob}\sin\theta_{ob} \\ & - (a_k - a_{k+1})y_{ob}\cos\theta_{ob} \\ & + (b_k - b_{k+1})x_{ob}\cos\theta_{ob} \\ & - a_k b_{k+1} + a_{k+1}b_k, \qquad i = 1, \ldots, n_f. \end{aligned} \tag{A.15}$$

During manipulation, the object may be stable in either form closure or force closure. These possibilities lead to two interpretations of each constraint. If there are three contacts (force closure), then only the object's position given by x_{ob}, y_{ob}, and θ_{ob} must be found. For the case of four contacts (form closure), the choice of the finger angles is not free. The specified quantities are x_p, y_p, θ_p, and θ_i, $i = 1, \ldots, n_f - 1$. The remaining variables, θ_{n_f}, x_{ob}, y_{ob}, and θ_{ob}, are determined by solving the four constraint equations.

References

Boissonnat, J. D. 1982. Stable matching between a hand structure and an object silhouette. *IEEE Trans. Pattern Analysis Machine Intelligence.* PAMI-4 (6):603-612.

Brost, R. C. 1985. Planning robot grasping motions in the presence of uncertainty. CMU-RI-TR-85-12. Pittsburgh: The Robotics Institute, Carnegie-Mellon University.

Cutkosky, M. R. 1985. *Robotic grasping and fine manipulation.* Boston: Kluwer Academic.

Featherstone, R. 1985 (Gouvieux, Oct. 7-11). The dynamics of rigid body systems with multiple concurrent contacts. *Proc. Third Intl. Symp. on Robotics Research:* 24-31.

Gill, P. E., Murray, W., and Wright, M. H. 1981. *Practical optimization.* New York: Academic Press.

Greyville, T. N. E. 1959. The pseudoinverse of a rectangular or singular matrix and its applications to the solutions of systems of linear equations. *SIAM Rev.* 1(1):38-43.

Hanafusa, H. and Asada, H. 1982. A robot hand with elastic fingers and its application to assembly process. In *Robot motion,* ed. M. Brady *et al.,* pp. 337-359. Cambridge, Mass.: MIT Press.

Hanafusa, H. *et al.* 1985 (Tokyo). Structural analysis and robust prehension of robotic hand-arm system. *Proc. Intl. Conf. on Advanced Robotics:* 311-318.

Holzmann, W. and McCarthy, J. M. 1985 (St. Louis, March 18-21). On grasping planar objects with two articulated fingers. *Proc. IEEE Intl. Conf. on Robotics and Automation:* 576-581.

Jameson, J. W. 1985. Analytic techniques for automated grasping. Ph.D. Dissertation, Stanford University.

Juan, J. and Paul, R. P. 1986 (San Francisco, April). Planning automatic assembly for robots (PAAR). *Proc. IEEE Intl. Conf. on Robotics and Automation.*

Kerr, J. R. 1984. An analysis of multi-fingered hands. Ph.D. Dissertation, Stanford University.

Kobayashi, H. 1984 (Kyoto, August 20-23). On the articulated hands. *Second Intl. Symp. on Robotics Research:* 128-135.

Kuan, D. T., Zamiska, J. C., and Brooks, R. A. 1985 (St. Louis, March 18-21). Natural decomposition of free space for path planning. *Proc. IEEE Intl. Conf. on Robotics and Automation:* 168-173.

Lakshminarayana, K. 1978. Mechanics of form closure. *ASME Report No. 78-DET-32.*

Laugier, A. C. and Pertin, A. J. 1983. Automatic grasping: A case study in accessibility analysis. Report 342. Toulouse, France: Laboratoire d'Informatique Fondamentale et d'Intelligence Artificielle.

Lemarechal, C. and Mifflin, R. 1977. *Nonsmooth optimiza-*

tion: Proceedings of the IIASA Workshop. New York: Pergamon Press.

Mason, M. T. 1984 (Kyoto, August 20–23). Mechanics of pushing. *Second Intl. Symp. on Robotics Research:* 73–80.

Mason, M. T. and Salisbury, J. K., Jr. 1985. *Robot hands and the mechanics of manipulation.* Cambridge, Mass.: MIT Press.

Nguyen, V. 1985. The synthesis of force closure grasps in the plane. TR-861, Massachusetts Institute of Technology Artificial Intelligence Laboratory.

Okada, T. 1982. Computer control of multijointed finger system for precise object-handling. *IEEE Trans. Systems, Man, Cybernet.* SMC-12 (3):289–298.

Paul, R. P. 1981. *Robot manipulators: mathematics, programming, and control.* Cambridge, Mass.: MIT Press.

Reuleaux, A. F. 1963. *The kinematics of machinery.* New York: Dover.

Salisbury, J. K. 1982. Kinematic and force analysis of articulated hands. Ph.D. Dissertation, Stanford University, Department of Mechanical Engineering, STAN-CS-82-921.

Toussaint, G. T. 1984. Movable separability of sets. SOCS-84.17, Montreal: McGill University.

Trinkle, J. C. 1985. Frictionless grasping. MS-CIS-85-46, GRASP Lab 52. Philadelphia: University of Pennsylvania, General Robotics and Active Sensory Perception Laboratory.

Whittaker, E. T. 1937. *Analytical dynamics.* Cambridge: Cambridge University Press.

Wolter, J. D., Volz, R. A., and Woo, A. C. 1984. Automatic generation of gripping positions. Technical Report, Ann Arbor: University of Michigan.